ELSEVIER

Journal of Nuclear Materials 273 (1999) 171–176

journal of nuclear materials

www.elsevier.nl/locate/jnucmat

Chemical interactions in the EXOTIC-7 experiment

H. Kleykamp *

Forschungszentrum Karlsruhe, Institut für Materialforschung I, Postfach 3640, 76021 Karlsruhe, Germany

Received 4 November 1998; accepted 20 January 1999

Abstract

Post-irradiation studies by X-ray microanalysis are reported on selected samples of the MANET steel lined capsule 28.2 of the EXOTIC-7 experiment within the fusion breeder blanket materials irradiation programme. A mixture of Be pebbles and SiO_2 doped Li_4SiO_4 pebbles with 52% ^6Li enrichment has been irradiated in the HFR up to 18% burn-up. A Li/Si decrease in the breeder material is observed due to Li transmutation which results in higher amounts of Li_2SiO_3 in the Li_4SiO_4 pebbles. Furthermore, oxygen is released which oxidises the surface of the Be pebbles to BeO. Direct BeO–Li_2SiO_3 contact leads to the formation of Li_2BeSiO_4. The predominant Li_2O vapour species is transported to the colder, inner liner surface of the pebble bed and recondenses as stratified Li_2O and Li_8SiO_6 layers. The chemical reactions between the MANET steel liner and the breeder materials play a minor role.

1. The irradiation experiment EXOTIC-7

The irradiation experiment EXOTIC-7 represents the first in-pile test on Li_4SiO_4 pebbles with 52% ^6Li enrichment and DEMO relevant burn-ups. The material was partly mixed with beryllium pebbles and was irradiated in three austenitic steel capsules (No. 26.2, 28.1 and 28.2) in the high flux reactor (HFR) Petten in the period February 1994 to February 1995. Other ceramic breeder materials irradiated simultaneously in the remaining five capsules were $LiAlO_2$, Li_8ZrO_6 and Li_2ZrO_3 pellets and Li_2ZrO_3 pebbles. The capsule No. 28.2 with dimensions 11 mm diameter and 80 mm height was fitted with an inner liner of ferritic/martensitic MANET steel. The maximum burn-up was 18% related to the total lithium. The capsule contained 0.1–0.2 mm diameter Li_4SiO_4 pebbles with an excess of 1.4% SiO_2 and Be pebbles with diameters of 0.1–0.2 and 2 mm. The mass ratio Li_4SiO_4 : Be was about 1:5. The irradiation temperatures were quoted by 410–480°C. The central and the surface temperatures of the capsule measured by thermocouples changed during the total irradiation period. However, the time-average temperature gradient was about 30 K [1].

The 2 mm Be pebbles were separated after irradiation by sieving before further metallographic treatment of the irradiated blanket material. Therefore, the pebble arrangement is not the original state during irradiation. A light-optical micrograph of the embedded 0.1–0.2 mm Li_4SiO_4 and Be particles is presented in Fig. 1. The dark grey ceramic phase is partly broken. The letters A and D designate the positions of detailed investigations. A further metallographic cross-section of the MANET liner with adherent blanket material was prepared especially for X-ray microanalysis in order to analyse possible incompatibilities of Be and Li_4SiO_4 with the steel. The numbers 1 and 2 in Fig. 2 designate the regions of detailed investigations. The total results are reported in Ref. [2].

2. X-ray microanalysis

Qualitative and quantitative chemical analyses in μm areas were done on two metallographic sections (Figs. 1 and 2) using the shielded X-ray microanalyser Jeol JRXA-50/JSM 6400 of IMF I in the Hot Cells of the Centre. For this purpose, a special diffraction crystal had been installed in one of the X-ray spectrometers

* Corresponding author. Tel.: +49-7247 82 2888; fax: +49-7247 82 4567; e-mail: heiko.kleykamp@imf.fzk.de

0022-3115/99/$ – see front matter
PII: S0022-3115(99)00027-6

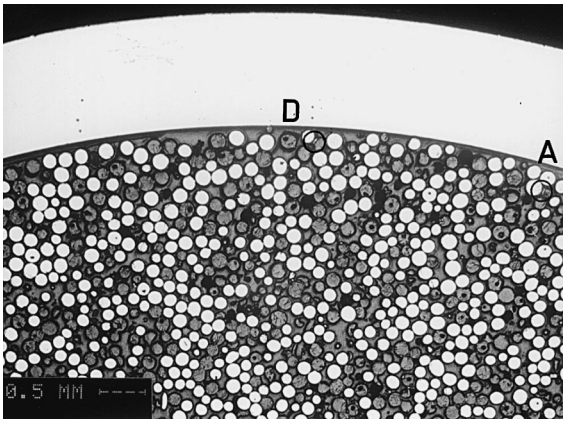

Fig. 1. Light-optical micrograph of the sieved 0.2 mm diameter fraction of the Li_4SiO_4 and Be pebbles irradiated in capsule 28.2 of the EXOTIC-7 experiment. The metallic ring is a support for the embedding procedure.

which facilitates the direct Be analysis. The synthetic Mo–B_4C multilayer crystal in its final version has a lattice spacing $2d = 22.2$ nm and a spectral resolution $\Delta\lambda/\lambda = 0.066$. A full width at half maximum $\Delta E = 7.2$ eV and a detection limit $c_{\min} = 0.2\%$ for Be Kα radiation ($\lambda = 11.35$ nm) in Be were measured under optimised conditions [3].

Two-dimensional element distribution images and quantitative point analyses can be taken in the element region between beryllium and uranium. Lithium cannot be measured directly. However, the remainder of the sum of the measured relative X-ray intensities of the heavier elements to 100% was taken for the calculation of the mass concentration of Li using a modern ZAF-correction program. This one converts the measured relative X-ray intensities I_i/I_{i0} where I_{i0} are the X-ray counts of a standard, to mass fractions c_i of the components i ($i = 1,\ldots,n$) in the respective phase.

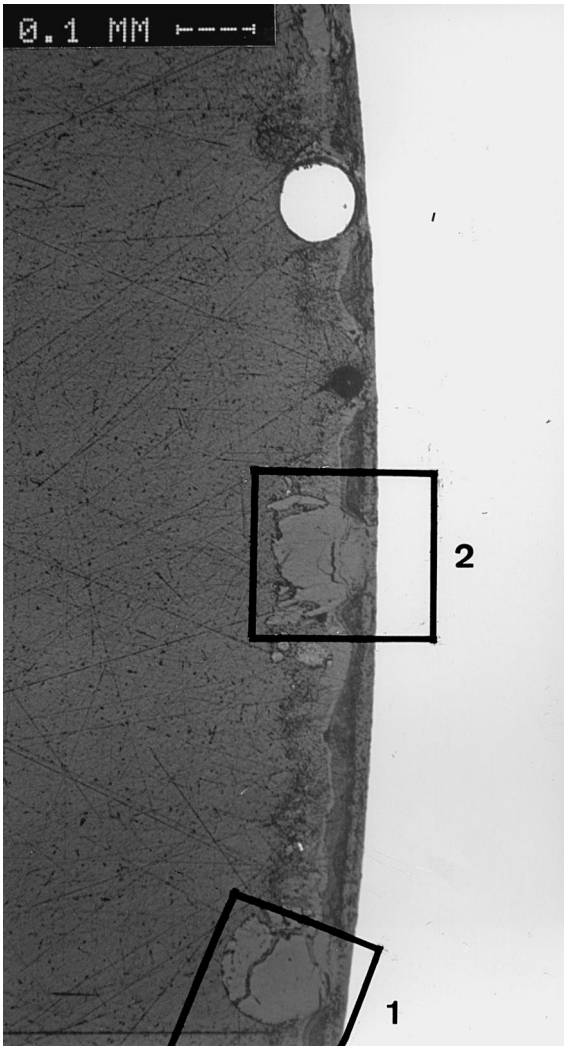

Fig. 2. Light-optical micrograph of two Li_4SiO_4 pebbles adjacent to the MANET liner in capsule 28.2 of the EXOTIC-7 experiment. The locations of the analysed regions 1 and 2 are given.

3. Results

3.1. Behaviour of Be and Li_4SiO_4 pebbles and their interactions

The Be pebbles are characterised by an about 30 μm thick porous outer zone, possibly due to the direct He and T recoil from the Li transmutation in the adjacent Li_4SiO_4 pebbles (Fig. 3). The quantitative analysis in the dense regions of the Be pebbles has shown that the Be mass concentration is about 97%, heavier elements are absent; therefore, the remainder of $\leqslant 3\%$ could be the elements H and He. The Be pebbles are further surrounded by a BeO layer up to 5 μm in thickness. In the case of direct contact of Be and Li_4SiO_4 during the irradiation period, a two-phase reaction layer about 30 μm in thickness formed. The reaction zone consists of the composition $Li_2Be_2O_3$ on the Be rich side and of Li_2BeSiO_4 on the Li_4SiO_4 side. The lower Si concentration in the quaternary phase compared to that in pure Li_4SiO_4 is reflected in the minor Si intensity on the right hand side of the Si distribution image in Fig. 3. The presentation of a two-dimensional Be distribution image is difficult in the presence of oxygen in the respective phase due to the high mass absorption coefficient of Be Kα radiation in oxygen. Therefore, the Be detection in an oxide phase is only possible by point analysis under a reduced working voltage 5 kV [3]. The different Be containing oxide phases are characterised by their grey

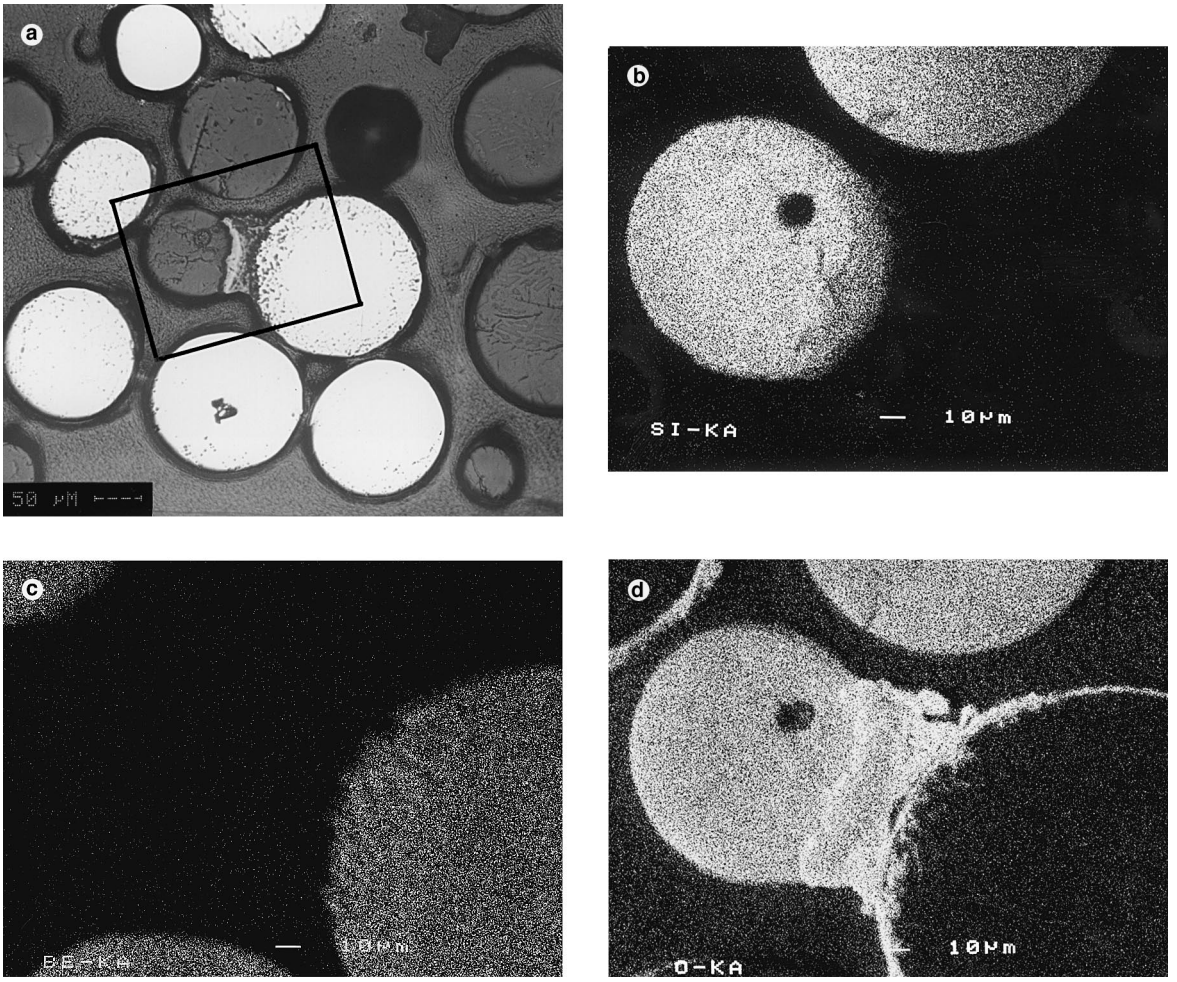

Fig. 3. Light-optical micrograph detail (a) of the interaction of a Li_4SiO_4 and a Be pebble, and Si (b), Be (c) and O (d) element distribution images; region A in Fig. 1.

value in the back-scattered electron image. The darker the phase, the lower is the average atomic number of the phase. The Si intensity in the Li_4SiO_4 pebbles is higher than in the Li_4SiO_4 standard indicating a substantial fraction of a Si richer phase, e.g. Li_2SiO_3, in these pebbles. A second example of a Be–Li_4SiO_4 interaction zone is presented in Fig. 4. The secondary electron image includes the numbers 1–6 where quantitative analyses were made in the respective phases.

3.2. Behaviour of Li_4SiO_4 near the cladding

The microstructure of the Li_4SiO_4 pebbles and their vicinity near the MANET liner (regions 1 and 2 in Fig. 2) observed by light-optical microscopy evidences a stratified structure of phases parallel to the cladding tube. The absorbed electron image (AEI) in Fig. 5 illustrates these layers C, E and G adjacent to the broken Li_4SiO_4 pebble A and to the MANET steel F. The phases are in essence Li_8SiO_6 and Li_2O. Iron plays a minor role in the phase formation. The results are compiled in Table 1. The same behaviour is reflected in the absorbed electron image and in the element distribution images in Fig. 6. Positions A and B of the quantitative analysis represent the broken Li_4SiO_4 pebble in the burnt state; positions C, D and E indicate the stratified layers parallel to the cladding which again consist of Li_8SiO_2 and Li_2O, resp. The results of the quantitative analysis are compiled in Table 2.

The microstructures show further Be pebbles near the MANET liner separated by stratified layers. Two different phases were formed which are composed of Li_2O and $Li_2(Fe)O$. The measured Fe concentration is too low to suppose the composition Li_5FeO_4 which is in equilibrium with $Li_2(Fe)O$ and Fe. This Fe containing phase is the only product of a chemical breeding material-

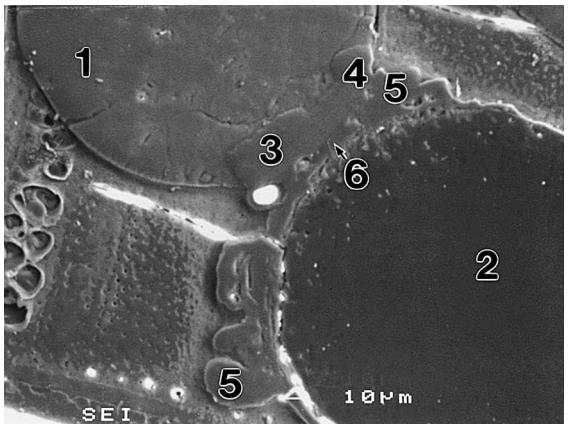

Fig. 4. Secondary electron image of the Li_4SiO_4–Be interaction zones, region D in Fig. 1. The numbers represent the positions of the quantitative analysis: (1) Li_4SiO_4–Li_2SiO_3 (two-phase); (2) $\geqslant 97\%$ Be (remainder: H and He); (3, 4) Li_2BeSiO_4; (5) $Li_2Be_2O_3$; (6) BeO.

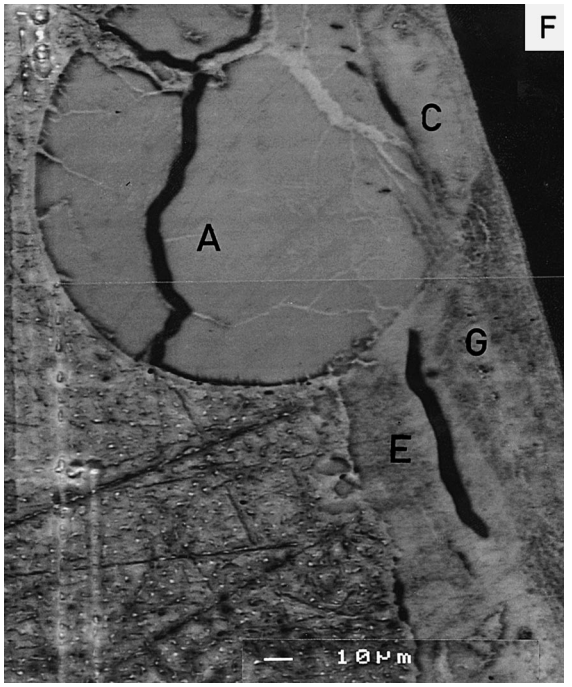

Fig. 5. Absorbed electron image (AEI) of a Li_4SiO_4 pebble (A) and different phases (C, E, G) adjacent to the MANET liner (F) illustrated in Fig. 2, region 1, see Table 1.

cladding interaction. In order to quantify the reaction layer sequence between the MANET liner and the Be pebble, concentration profiles were made perpendicular to the inner liner surface region. The profiles of selected elements were recorded as ZAF-corrected step scans. The sequence of the phases is as follows:

Table 1
Composition of the phases A, C, E and G adjacent to the MANET liner in Fig. 5

Position	Concentration in at.%				Phases
	O	Si	Fe	Li (balance)	
A	45	16	0.03	39	Li_4SiO_4 Li_2SiO_3
C	33	7	0.2	60	Li_8SiO_6
E	>30	0	0	–	$\approx Li_2O$
G	39	0.06	5	56	$Li_2(Fe)O$

- MANET liner with about 0.25% Si, 85% Fe, 11% Cr,
- $Li_{2-x-y}Fe_xCr_yO$, $x \gg y$,
- Li_2O,
- BeO,
- Be.

The principal phase between the liner and the Be pebble is Li_2O.

4. Discussion

Out-of-pile incompatibility studies between Be and Li_4SiO_4 have shown that a reaction layer of about 10 μm thickness and unknown composition formed at 650°C after 1000 h reaction time under argon [4]. According to the phase diagram of the quaternary Li–Be–Si–O system the formed reaction products should be $Li_2Be_2O_3$, BeO and Li_2Si [5]. The situation is different during irradiation of Li_4SiO_4 because the composition of the breeding material changes continuously. Li is transmutated to become T and He, the generated SiO_4^{-4} radicals form in part Li_2SiO_3 with the remaining Li_4SiO_4, and oxygen is released. The excess oxygen increases the chemical potential of oxygen and oxidises the generated tritium in the gas phase. The reactions are represented by the following equation at 18% burn-up disregarding a T–H exchange with the He–0.1 vol.% H_2 purge gas:

$$100\ Li_4SiO_4 \rightarrow 64\ Li_4SiO_4 + 36\ Li_2SiO_3 + 72\ He + 36\ T_2O. \quad (1)$$

The situation is more complicated in the presence of metallic Be. As oxygen has a higher affinity to Be than to hydrogen the following reaction takes place, again at 18% burn-up in the course of which Be is oxidised on free Be surfaces by reaction with the released oxygen:

$$100\ Li_4SiO_4 + 36\ Be \rightarrow 64\ Li_4SiO_4 + 36\ Li_2SiO_3 + 72\ He + 36\ T_2 + 36\ BeO. \quad (2)$$

BeO and Li_2SiO_3 are not in thermodynamic equilibrium. Therefore, a secondary reaction occurs in direct contact of both phases:

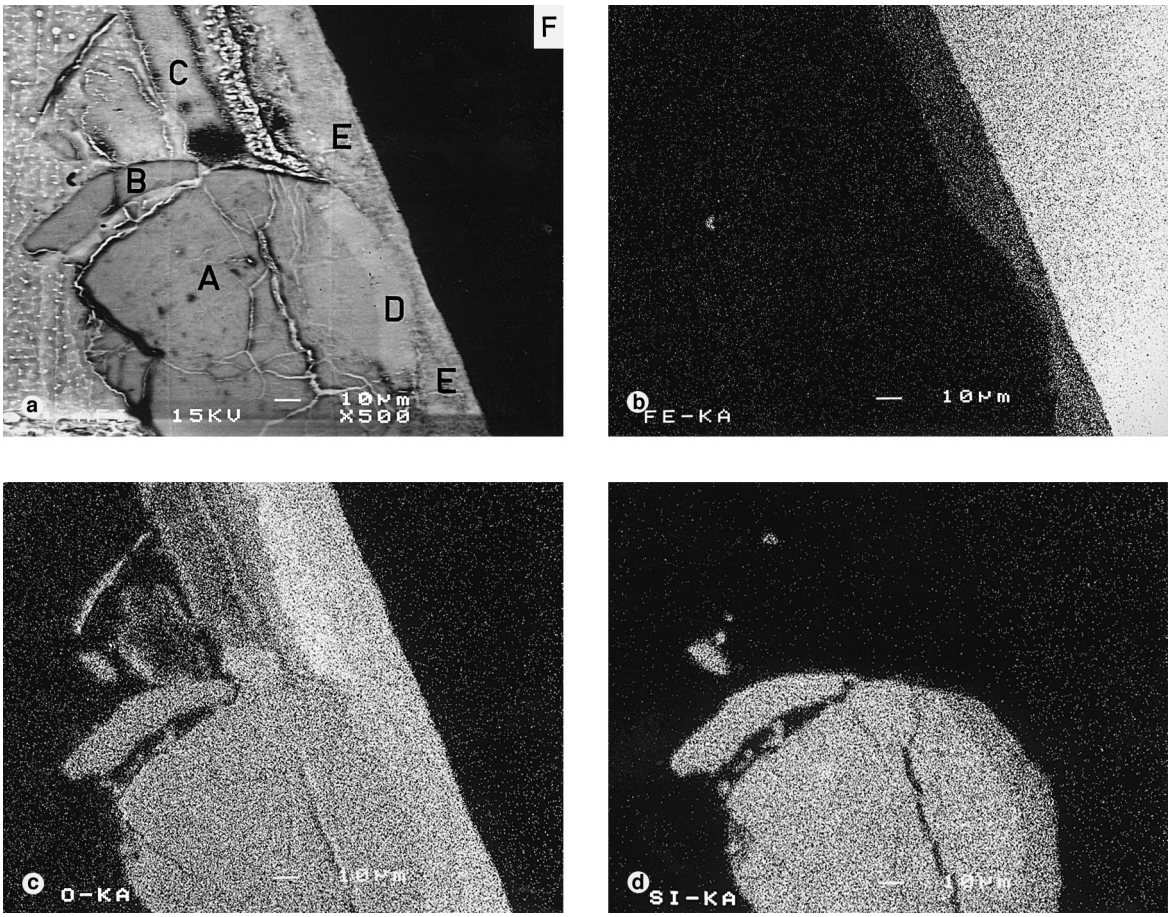

Fig. 6. Absorbed electron image and Fe, O and Si element distribution images of a Li_4SiO_4 pebble and phases adjacent to the MANET liner (F) in Fig. 2, region 2, see Table 2.

$$BeO + Li_2SiO_3 \rightarrow Li_2BeSiO_4. \quad (3)$$

This phase was observed as a reaction product in the EXOTIC-7 irradiation experiment. Single-phase Li_4SiO_4 pebbles have not been used but material with an excess of 1.4 mass% SiO_2 in order to increase the compressive strength of the pebbles, corresponding to 66.0 mol% Li_2O and 34.0 mol% SiO_2. This two-phase Li_4SiO_4–Li_2SiO_3 composition is not in thermodynamic equilibrium with BeO, but the phase Li_2BeSiO_4 is formed already at zero burn-up.

Another phenomenon occurs in a temperature gradient. Fission and transmutation processes in materials within a radiation field result in a temperature gradient in the direction of the centre of this material which is followed by mass transport of the high vapour pressure components Li, Li_2O and O_2 via the gas phase to lower temperatures. The volatile gas species condense at the lowest temperatures on the inner surface of the MANET liner. The different phases are formed in a stratified arrangement. The phase with the highest vapour pressure is positioned at the lowest temperature.

The following reaction scheme is assumed, $\langle \ldots \rangle$ means a solid phase, e.g. $\langle Li_4SiO_4 \rangle$, $(\ldots)$ means a gaseous phase, e.g. (Li_2O):

Table 2
Composition of the phases A, B, C, D and E adjacent to the MANET liner in Fig. 6

Position	Concentration in at.%				Phases
	O	Si	Fe	Li (balance)	
A	28	14	0.04	58	Li_4SiO_4 Li_2SiO_3
B	26	15	0.03	59	Li_8SiO_6 Li_4SiO_4
C	>30	0	0	–	$\approx Li_2O$
D	36	7	0.07	58	Li_8SiO_6
E	34	0	4	62	$Li_2(Fe)O$

$\langle Li_4SiO_4\rangle = 2(Li_2O) + \langle SiO_2\rangle$, evaporation,

$\langle SiO_2\rangle + \langle Li_4SiO_4\rangle = 2\langle Li_2SiO_3\rangle$, solid state reaction.

Gaseous Li_2O is transported to lower temperatures; the following reactions occur in this region:

$2(Li_2O) + \langle Li_4SiO_4\rangle = \langle Li_8SiO_6\rangle$, recondensation,

$\langle Li_8SiO_6\rangle = 4(Li_2O) + \langle SiO_2\rangle$, evaporation,

$\langle SiO_2\rangle + \langle Li_8SiO_6\rangle = 2\langle Li_4SiO_4\rangle$, solid state reaction,

$4(Li_2O) = 4\langle Li_2O\rangle$, recondensation.

The stratified Li_2O and Li_8SiO_6 phases were indeed observed parallel to the MANET liner and adjacent to the Li_4SiO_4 pebble according to the Li_2O–Li_8SiO_6–Li_4SiO_4 sequence of the phases in the quasi-binary Li_2O–SiO_2 system. The Cr and Fe oxidation plays a minor role. These oxides react with Li_2O to $Li_{2-x-y}Fe_xCr_yO$. A quantitative analysis of this phase was not possible.

5. Conclusions

The experimental results reflect three effects which are well known from the post-irradiation studies on oxide fuels for fission reactors:

- The stoichiometry shift of the breeding material, i.e. the formation of Li_2SiO_3 from Li_4SiO_4 during irradiation.
- The oxidation of materials with high affinity to oxygen due to the irradiation induced oxygen release.
- Redistribution of components of the breeding material in the in-pile temperature gradient by evaporation–recondensation mechanisms.

The portion of the second, mostly Li containing phases in ceramic breeder materials (e.g. Li_2SiO_3 in Li_4SiO_4, ZrO_2 in Li_2ZrO_3, $Li_4Ti_5O_{12}$ in Li_2TiO_3) increases continuously with the transmutation progress. They have a different tritium release behaviour than the initial phases. The temperature gradient in the blanket canisters induces a macroscopic mass separation resulting in the redeposition of the phases with the highest vapour pressure in the regions of the lowest temperatures. Therefore, it would be advisable to incorporate these experimental results in the modelling processes of tritium release from ceramic breeder materials.

Acknowledgements

The author gratefully acknowledges the preparation of the metallographic sections by Mr E. Kaiser, G. Weih and F. Weiser of the Hot Cells and the X-ray microanalysis by Mr H.D. Gottschalg of IMF I of Forschungszentrum Karlsruhe.

References

[1] J.G. van der Laan, M. Stijkel, R. Conrad, Proc. 19th Symp. on Fusion Technol., Lisbon, 1996, p. 1511.
[2] H. Kleykamp, Chemical interactions in the EXOTIC-7 experiment, 7th Int. Workshop on Ceramic Breeder Blanket Interactions, Petten, The Netherlands, 1998.
[3] H. Kleykamp, Quantitative X-ray microanalysis of beryllium using a multilayer diffracting device, 15th Int. Congr. on X-ray Optics and Microanalysis, Antwerp, Belgium, 1998.
[4] P. Hofmann, W. Dienst, J. Nucl. Mater. 171 (1990) 203.
[5] H. Migge, Proc. 14th Symp. on Fusion Technol., Avignon, 1986, p. 1209.